Understanding Nitric Acid–Induced Changes in the Arrangement of Monomeric and Polymeric Methacryloyl Diglycolamides on Their Affinity toward f-Element Ions

ARTICLE *in* THE JOURNAL OF PHYSICAL CHEMISTRY B · DECEMBER 2014

Impact Factor: 3.3 · DOI: 10.1021/jp510170v · Source: PubMed

THE JOURNAL OF PHYSICAL CHEMISTRY B

Article

pubs.acs.org/JPCB

Understanding Nitric Acid-Induced Changes in the Arrangement of Monomeric and Polymeric Methacryloyl Diglycolamides on Their Affinity toward f-Element Ions

Vivek Chavan,[†] Sabyasachi Patra,[†] Ashok K. Pandey,*[,†] Vasudevan Thekkethil,[‡] Mudassir Iqbal,[∥] Jurriaan Huskens,[∥] Debasis Sen,[§] S. Mazumder,[§] Asok Goswami,[†] and Willem Verboom*[,∥]

[†]Radiochemistry Division, [‡]Research Reactor Services Division, and [§]Solid State Physics Division, Bhabha Atomic Research Centre, Trombay, Mumbai-400085, India

[∥]Laboratory of Molecular Nanofabrication, MESA+ Institute for Nanotechnology, University of Twente, P.O. Box 217, 7500 AE Enschede, The Netherlands

Supporting Information

ABSTRACT: Assembled diglycolamides (DGAs) have a strong affinity toward f-element ions at high nitric acid concentrations. Small angle X-ray scattering studies revealed that nitric acid concentration dependent changes occur in the geometrical arrangement of the DGA units of monomeric methacryloyl-DGA and the corresponding polymeric DGA. Cylindrical aggregates of methacryloyl-DGA were formed in 10:1 *n*-dodecane:1-decanol (added for solubility reasons) upon equilibration with nitric acid. The lengths and diameters of the cylindrical methacryloyl-DGA aggregates increased on varying the nitric acid concentration from 3 to 4 mol L^{-1}. This resulted in an increase of the distribution coefficient (D) of Eu^{3+} ions from 72 to 197. The physical structure of cross-linked (10 mol %) poly(methacryloyl-DGA) reorganized distinctly upon equilibration with nitric acid. In this case, also the $D_{Eu^{3+}}$ values increased significantly from 147 mL g^{-1} at 1 mol L^{-1} HNO_3 to ~4000 mL g^{-1} at 4 mol L^{-1} HNO_3. Hydrogen bonds between the outer sphere of Eu^{3+}/Am^{3+}/Pu^{4+} nitrate and DGA units provide stabilization in the hydrophobic environment. This results in enhancement of their extraction upon increasing nitric acid concentration both in the organic phase as well as in the polymer matrix. Though monomeric and polymeric methacryloyl-DGA are different in their physical assembling, the normalized D_I values for a same f-element ion upon varying HNO_3 concentrations show remarkably similar patterns in both forms. In addition, the unusual stoichiometry deduced from the slopes of the log D vs log[HNO_3] curves at fixed nitrate concentration seems to suggest that the normal extraction mechanism may not be operating in the hydrogen bonded DGA assemblies.

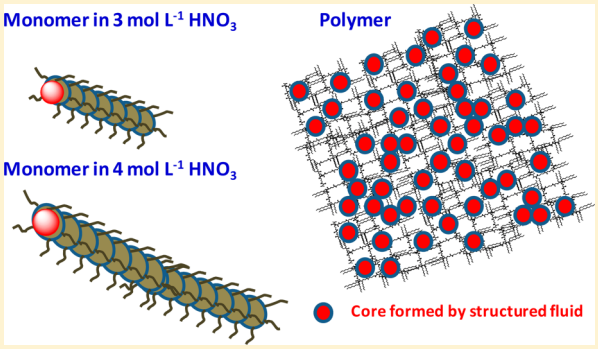

INTRODUCTION

Diamides are a very promising group of extractants for partitioning of tri- and tetravalent ions of f-elements from solutions containing high concentrations of nitric acid.[1] The diamide bridges that make a diamide to chelate with f-elements are either alkyl groups (malonamides or succinamides), an ether oxygen (diglycolamides), or a sulfur atom (thiadiglycolamides).[2,3] The affinity of a diamide toward f-element ions is dependent not only on the molecular structure of the bridge between the two amide groups but also on the nitric acid-induced aggregation of the diamide ligands.[4−6] Among several diglycolamides studied, *N*,*N*,*N*′,*N*′-tetraoctyldiglycolamide (TODGA) has been found to be the best extractant for the partitioning of minor actinides both in terms of the solubility in *n*-dodecane and the extractability toward Ln(III) and An-(III,IV) from highly acidic solutions.[7−9]

Slope analysis of the distribution coefficients (D) of An(III) in TODGA−*n*-dodecane as a function of the nitric acid concentration revealed that the apparent number of nitrate anions participating in the extraction is ~6 at higher nitric acid concentrations.[10] That is considerably higher than required to balance the positive charge of the An^{3+} cation. There is no possibility of extraction of anionic or cationic An(III) complexes by a neutral extractant like TODGA. Therefore, this "hyperstoichiometric" nitrate dependence could only be explained on the basis of the extraction of neutral $An(NO_3)_3 \cdot 3HNO_3$ complex species. However, the extraction of An(III) in this form seems to suggest the involvement of another physical process in the extraction of An(III) with TODGA.

Small angle X-ray scattering (SAXS) studies have revealed that formation of reverse micelles by amphiphilic extractants in an organic phase influences the solvent extraction process in

Received: July 5, 2014
Revised: December 1, 2014
Published: December 11, 2014

DOI: 10.1021/jp510170v
J. Phys. Chem. B 2015, 119, 212−218

terms of complexation and third phase formation.[11−15] Ellis et al. have studied Ln coordination and the formation of supramolecular assemblies in malonamide solvent extraction systems using SAXS.[16,17] They observed the coagulation of reverse micelles into worm-like aggregates in organic phases (*N*,*N*′-dimethyl-*N*,*N*′-dibutyltetradecylmalonamide in *n*-dodecane) equilibrated with an aqueous medium containing trivalent cerium.[16] They have also shown that the coordination chemistry of lanthanides within nanoconfined environments in the cores of the reverse micelles containing water, nitric acid, and extractant is equivalent neither to the solid nor the bulk solution behaviors.[17] It has been observed that the larger, more hydrated, acidic core of a reverse micelle favors monodentate, whereas the small, dry, neutral core favors bidentate nitrate coordination to Ln(III).[17] Studies involving small angle neutron scattering (SANS), SAXS, and vapor pressure osmometry (VPO) showed that diglycolamides in the organic phase also form reverse-micelle-type supramolecular aggregates upon equilibration with nitric acid solutions. This explains the involvement of four diglycolamide units and three to six nitrate ions in the complexation with an An(III) ion.[10,18−20] SANS studies carried out by Pathak et al. have indicated that the aggregate size increases with increasing acidity and goes beyond the formation of tetramers at 6 mol L^{-1} nitric acid (n = 8.2).[21] On the basis of these studies, DGA groups have been preorganized on trialkylphenyl and calix[4]arene platforms and also as bisdiglycolamide, giving rise to enhanced extraction of Am(III) and Eu(III).[22−24] Recently, a DGA-containing silica resin has been synthesized, which has been found to be quite efficient for actinide(III,IV) extraction in a similar way as diglycolamide extractants.[25] It is interesting to note that polymeric DGA formed by using *N*,*N*-dioctyl,*N*′-propyl-2-methylacrylamide diglycolamide (methacryloyl-DGA) as a monomer showed a similar behavior, although nitric acid-induced aggregation is not expected in a cross-linked polymeric form.[26]

The present work deals with a study on the changes in the geometrical arrangement of the aggregates of asymmetric methacryloyl-DGA and poly(methacryloyl-DGA) upon equilibration with nitric acid using SAXS to understand the sorption/desorption behavior of Ln(III)/An(III,IV,VI) in the different spatial arrangements of DGA groups. To study the effect of the changes in the aggregates on the extraction ability, extraction studies were carried out with methacryloyl-DGA and TODGA (Scheme 1) in a 10:1 mixture of *n*-dodecane and 1-decanol and cross-linked poly(methacryloyl-DGA) for Eu^{3+}, UO_2^{2+}, Am^{3+}, and Pu^{4+} as the representative f-element ions.

Scheme 1. Chemical Structures of (a) TODGA and (b) Methacryloyl-DGA

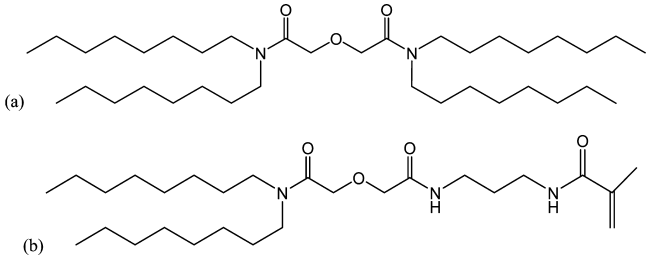

EXPERIMENTAL SECTION

Details of the syntheses of methacryloyl-DGA and poly(methacryloyl-DGA) (cross-linked with 10 mol % of ethylene glycol dimethacrylate with respect to monomer) are given in our earlier publication.[26] Liquid−liquid extractions were carried out by equilibrating 0.5 mL of an organic phase containing the desired concentration of extractant (TODGA/methacryloyl-DGA) with the same volume of an aqueous phase containing the required amount of ^{241}Am and concentration of HNO_3. The organic phases consisted of methacryloyl-DGA (0.05 mol L^{-1}) or TODGA (0.01 mol L^{-1}) dissolved in a 10:1 mixture of *n*-dodecane and 1-decanol. The nitric acid concentration was kept the same as that used for pre-equilibrating the organic phase. The equilibrations were carried out for 30 min at room temperature with constant shaking in a temperature bath. After equilibration, the radioactivity of ^{241}Am or ^{154}Eu was measured in both the organic and aqueous phases by subjecting 0.3 mL samples to γ-spectrometry using a NaI(Tl) detector coupled to a multichannel analyzer. The α-radioactivity of $^{233}U/^{238,239,240}Pu$ was monitored by liquid scintillation counting as described elsewhere.[26] For the liquid−liquid extraction systems, the D values were obtained as the mean ratios (average of three experiments) of the radioactivity or concentration of $^{241}Am/^{154}Eu$ in the organic to that in the aqueous phase. The D value for a poly(methacryloyl-DGA)−aqueous phase system was obtained by

$$D = \frac{(C_0 - C_e)}{W} \times \frac{V}{C_e} \quad (1)$$

where C_0 and C_e represent the radioactivity of ^{241}Am initially and after equilibration in the aqueous phase and W and V are the weight of the poly(methacryloyl-DGA) and the volume of the aqueous phase, respectively.

SAXS experiments were performed using a laboratory-based SAXS instrument with Cu K_α as probing radiation. The radial averaged scattering intensity ($I(q)$) was obtained within a wave vector transfer ($q = 4\pi \sin(\theta)/\lambda$, where λ is the wavelength and 2θ is the scattering angle) range of ∼0.1 to 2.5 nm^{-1}. Solutions of methacryloyl-DGA and TODGA in the appropriate solvents (*n*-dodecane or a 10:1 mixture of *n*-dodecane and 1-decanol, equilibrated with the aqueous solution having 3 and 4 mol L^{-1} HNO_3 with or without Eu^{3+} ions (0.1 mol L^{-1})) in thin quartz capillaries (OD = 0.5 mm) were used for the scattering experiments. Background scattering from the blank capillary was subtracted from the SAXS data. As explained in the Supporting Information and shown in Figure S1, the scattering background from the solvent did not affect the functionality of the SAXS profiles significantly. This is due to the fact that the scattering cross section for solvent is low and is almost independent of the wave-vector transfer; e.g., it is ∼0.02 cm^{-1} for *n*-dodecane.[27]

While fitting the SAXS profiles with various standard models, it was realized that consideration of the form factor corresponding to anisotropic particle shape is quite appropriate in the present case. Therefore, the dilute cylindrical particle model was considered to fit the SAXS profiles.[28] This fits reasonably well with the data. The scattering intensity $I(q)$ from an ensemble of cylindrical particles is given by[28]

$$I(q) = CP(q) \quad (2)$$

DOI: 10.1021/jp510170v
J. Phys. Chem. B 2015, 119, 212−218

where $P(q)$ is the form factor of the cylindrical particles and C is a q independent scale factor, which depends on the scattering contrast, number density, and volume of the particles.

$$P(q) = \int_0^{\pi/2} \left[\frac{2J_1(qR\ \sin(\alpha))}{qR\ \sin(\alpha)} \frac{\sin(qL\ \cos(\alpha)/2)}{(qL\ \cos(\alpha)/2)} \right]^2 \sin(\alpha)\ d\alpha \quad (3)$$

Herein, $J_1(x)$ represents the first order Bessel function. R and L are the radius and the length of the cylinders, respectively. The integration over α takes into account all possible orientations of the cylinders in the dispersion. Monodisperse cylindrical particles were considered for the SAXS profiles of methacryloyl-DGA in the organic phases equilibrated with aqueous phases containing 3 and 4 mol L^{-1} HNO_3. It needs to be mentioned that the statistics of the scattering data obtained in the present work was not sufficient enough to estimate polydispersity unambiguously. Thus, the polydisperse cylinder model was intentionally avoided. Equation 2 was fitted to the experimental data using the nonlinear least-square method to estimate the radius and the length of the cylinders. For methacryloyl-DGA loaded with Eu^{3+}, the fittings of the low q regime (below 0.2 nm^{-1}) were different at different acidities (3 and 4 mol L^{-1}); see Figure 1. In the case of 3 mol L^{-1} acidity, the scattering profile in the low q region varied as q^{-4}; see Figure S2 (Supporting Information). Therefore, one extra term C'/q^4 was added to eq 2. Here C' represents the scale factor. However, at 4 mol L^{-1}, the increase of the scattering intensity significantly differs from the variation mentioned above. It could be best represented by introducing the interparticle structure factor in eq 2. In such a case, the scattering intensity $I(q)$ is given by

$$I(q) = CP(q)S(q) \quad (4)$$

In the present case, the structural factor $(S(q))$ corresponding to a fractal-like agglomerate was considered, as it could fit the data reasonably well.[29]

$$S(q) = 1 + \frac{1}{(qr_0)^{D_f}} \frac{D_f\Gamma(D_f - 1)}{[1 + 1/(q^2\xi^2)]^{(D_f-1)/2}} \sin[(D_f - 1)\tan^{-1}(q\xi)] \quad (5)$$

D_f is the mass fractal dimension, r_0 is the radius of the basic unit of the fractal, ξ is the upper cutoff, and $\Gamma(x)$ is the gamma function of argument x.

RESULTS AND DISCUSSION

Methacryloyl-DGA is insoluble in n-dodecane due to the absence of two C-8 hydrocarbon chains compared to TODGA; see Scheme 1. To make it soluble in n-dodecane, 1-decanol was added effecting aggregation in the form of reverse micelles. To study the geometrical arrangements of methacryloyl-DGA and TODGA in n-dodecane:1-decanol (10:1), SAXS experiments were carried out upon equilibration with 3 mol L^{-1} HNO_3-containing aqueous phases with or without Eu^{3+} ions. From the SAXS profiles shown in Figure S3 (Supporting Information), it was concluded that reverse micelle formation by TODGA does not occur even upon equilibration with 3 mol L^{-1} HNO_3, apparently due to the presence of the polar solvent 1-decanol. In n-dodecane, TODGA aggregates into spherical reverse micelles consisting of a core containing water and extracted

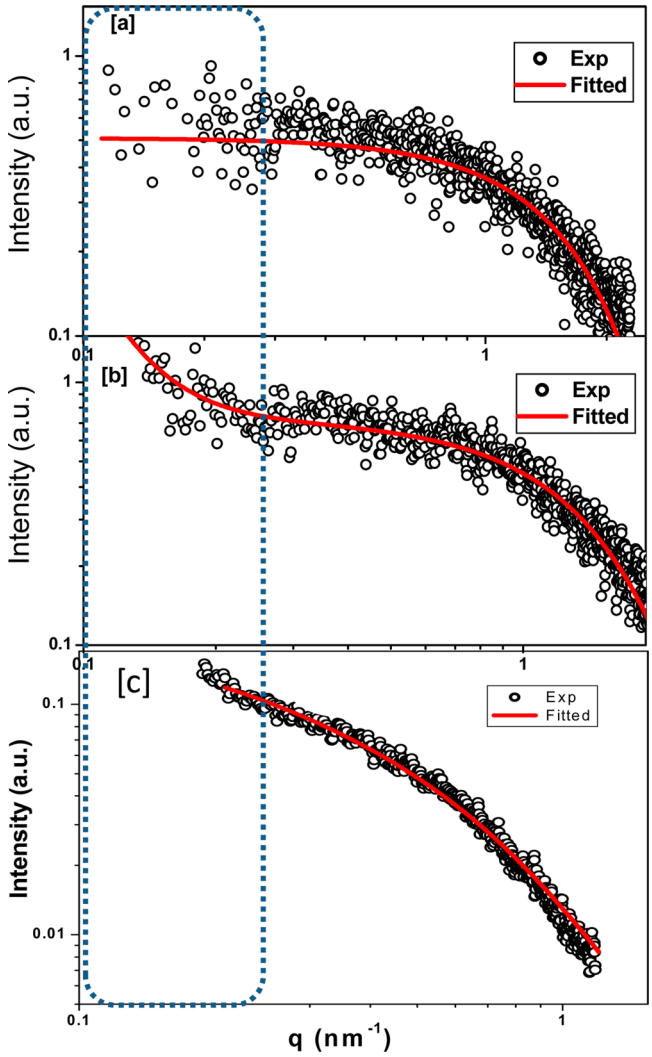

Figure 1. (a) SAXS profiles of methacryloyl-DGA in the organic phase (10:1 mixture of n-dodecane and 1-decanol) equilibrated with 3 mol L^{-1} HNO_3. SAXS profiles of Eu^{3+}-loaded methacryloyl-DGA in the organic phase equilibrated with (b) 3 mol L^{-1} HNO_3 and (c) 4 mol L^{-1} HNO_3.

ions surrounded by approximately four TODGA molecules.[10,18−20]

The SAXS profile of methacryloyl-DGA does show formation of reverse micelles. However, aggregation was not observed when the organic phase was not equilibrated with HNO_3 (Figure S3, Supporting Information). A noticeable change in the SAXS profile at low q (below 0.2 nm^{-1}) is observed upon loading with Eu^{3+} ions in a methacryloyl-DGA containing organic phase (see encircled portion of Figure 1), indicating the formation of bigger aggregates of reverse micelles.

The SAXS profiles of Eu^{3+}−methacryloyl-DGA at 3 and 4 mol L^{-1} HNO_3 could be fitted reasonably well with a cylindrical form factor. The formation of nonspherical reverse micelles can be attributed to the asymmetric chemical architecture of methacryloyl-DGA, as shown in Scheme 1. From the low q region (below 0.2 nm^{-1}) of the SAXS profiles given in Figure 1c, it can be concluded that the reverse micelles also aggregated upon Eu^{3+} loading at 4 mol L^{-1} HNO_3.

The dimensions of the cylindrical reverse micelles formed by methacryloyl-DGA calculated by analysis of the high q part of

DOI: 10.1021/jp510170v
J. Phys. Chem. B 2015, 119, 212−218

the SAXS profiles are given in Table 1. Interestingly, the length and diameter of the reverse micelles increased upon changing

Table 1. Comparison of Dimensions of Methacryloyl-DGA Aggregates Formed in the Organic Phase (*n*-Dodecane:1-Decanol = 10:1) Obtained from SAXS Studies as a Function of HNO_3 Concentration with Distribution Coefficient of Eu^{3+} Ions ($D_{Eu^{3+}}$)

HNO_3 (mol L^{-1})	length of cylinder (nm)	mean radius (nm)	$D_{Eu^{3+}}$
0	no aggregation		
3	3.2	1.1	72[a]
4	6.5	1.2	197

[a]Taken from ref 26.

the HNO_3 concentration from 3 to 4 mol L^{-1}. Extraction experiments showed that the $D_{Eu^{3+}}$ value also increased from 72 to 197 upon this increase of the HNO_3 concentration. It is expected that an increase in acidity will drive more water and acid in the organic phase. Since these are hydrogen bond promoting molecules (donor/acceptor), the increase in acidity in the system would lead to more hydrogen bonding in the core of the reverse micelles formed by the methacryloyl-DGA molecules.

Recently, Qiao et al. have studied the role of hydrogen bonding in Eu^{3+}-ion-containing reverse micelles formed by the amphiphilic extractant malonamide in *n*-heptane by means of atomistic molecular dynamics simulations and X-ray techniques.[30] They have shown that the growth of the reverse micelles in the form of swelling and elongation and the stabilization of $Eu(NO_3)_3$ are enhanced by increased hydrogen bonding under acidic conditions. The stabilization of $Eu(NO_3)_3$ in the hydrophobic environment of reverse micelles was attributed to hydrogen bonding between the outer sphere of a $Eu(NO_3)_3$ complex and aggregating amphiphiles.[30] The data in Table 1 show that swollen, elongated reverse micelles at 3−4 mol L^{-1} HNO_3 enhance the extraction of Eu^{3+} ions. This is consistent with the H-bonding hypothesis of Qiao et al.[30]

To understand the role of HNO_3 in the extraction of An^{3+} ions by DGAs, the variation of the distribution coefficient ($D_{Am^{3+}}$) of ^{241}Am as a function of the HNO_3 concentration was studied, keeping the total nitrate concentration fixed at 5 mol L^{-1} using NH_4NO_3. The plots of the log $D_{Am^{3+}}$ as a function of the log HNO_3 concentration for the different extraction systems are presented in Figure 2. In the case of TODGA in *n*-dodecane, the $D_{Am^{3+}}$ value increases continuously with the nitric acid concentration, and at high acidity, the slope changes to 5, indicating significant extraction of HNO_3 along with $Am(NO_3)_3$. In the 10:1 mixture of *n*-dodecane and 1-decanol, in which no aggregation takes place (vide supra) (see Figure S3, Supporting Information), the dependence of the $D_{Am^{3+}}$ value on the HNO_3 concentration is considerably reduced at lower acidity and almost disappears at higher acidity. This seems to suggest that the aggregation of TODGA plays a major role in the extraction process. In the case of methacryloyl-DGA, the $D_{Am^{3+}}$ values do not vary significantly up to the point (2.5 mol L^{-1} HNO_3) where the methacryloyl-DGA aggregates begin to form swollen and elongated structures. Thereafter, the $D_{Am^{3+}}$ values show a linear dependence on the HNO_3 concentration. This clearly indicates that HNO_3 plays a significant role by inducing H-bonding that stabilizes $Am(NO_3)_3$ complexes in the methacryloyl-DGA aggregates as explained above.

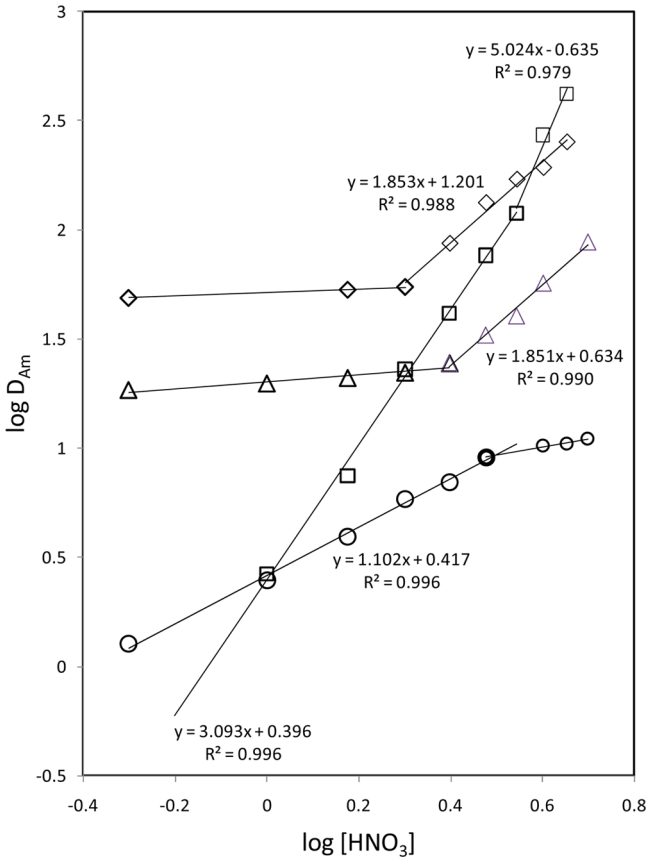

Figure 2. Plots of log $D_{Am^{3+}}$ versus log[HNO_3]. The nitrate concentration was kept constant at 5 mol L^{-1} using appropriate amounts of NH_4NO_3 and HNO_3. Symbols △, ○, □, and ◇ represent methacryloyl-DGA (0.05 mol L^{-1} in 10:1 *n*-dodecane and 1-decanol), TODGA (0.01 mol L^{-1} in 10:1 *n*-dodecane and 1-decanol), TODGA (0.01 mol L^{-1} in *n*-dodecane), and poly(methacryloyl-DGA), respectively. (In the latter case, the unit of $D_{Am^{3+}}$ is mL g^{-1}).

In Figure 2, it is interesting to see that the variation of log $D_{Am^{3+}}$ as a function of log[HNO_3] in the cross-linked poly(methacryloyl-DGA) has a similar trend as that in its monomeric form. This is unexpected, as the degree of cross-linking in poly(methacryloyl-DGA) was kept at 10 mol % to provide a higher network elasticity (rigidity). Poly-(methacryloyl-DGA) did also not contain liquid organic phase but was directly equilibrated with the acidic aqueous phase. Thus, the organization of polymer chains or the formation of reverse micellar structures is not expected. It is also important to note that Am^{3+} could not be deloaded from the poly(methacryloyl-DGA) matrix using the disodium salt of EDTA, while deloading from organic-phase-containing methacryloyl-DGA was rather easy.[26] In the case of DGA-grafted silica, the elution of Am(III) was also straightforward.[25]

To clarify this, the poly(methacryloyl-DGA) samples were treated with HNO_3 and subjected to SAXS analysis. From the SAXS profiles in Figure 3, it is clear that distinct changes in the physical structure of the poly(methacryloyl-DGA) matrix occur upon HNO_3 treatment. The radial averaged SAXS profile of the poly(methacryloyl-DGA) matrix before acid treatment shows an intense peak at scattering vector (q) = 2 nm^{-1}. This can be attributed to the interconnected morphology of the poly-(methacryloyl-DGA) matrix with a structural correlation. As the scattering space and the real space are connected by Fourier transform, the information about the smaller length scale is

DOI: 10.1021/jp510170v
J. Phys. Chem. B 2015, 119, 212−218

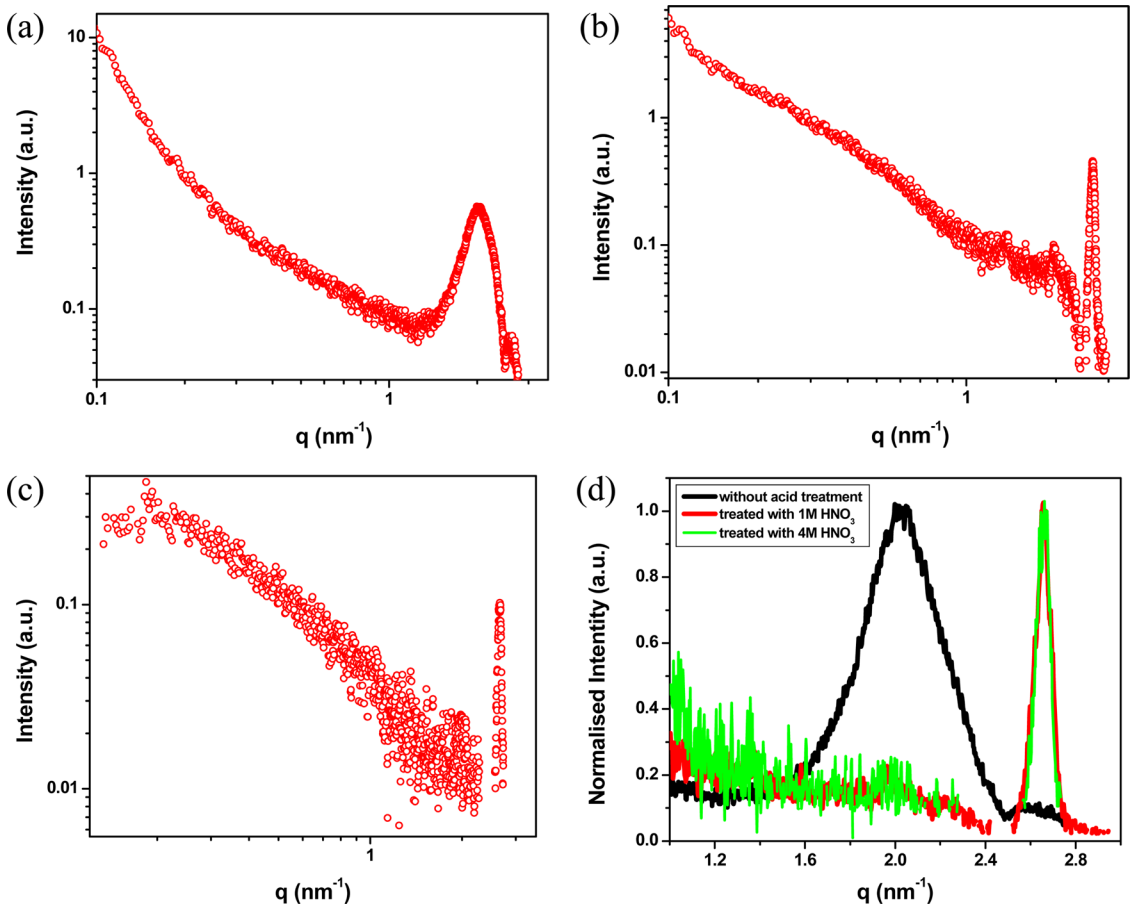

Figure 3. Radial averaged SAXS profiles of the poly(methacryloyl-DGA) matrix (a) before acid treatment, (b) after treatment with 1 mol L^{-1} HNO_3, and (c) after treatment with 4 mol L^{-1} HNO_3 and (d) normalized profiles of all three samples zoomed at a high q regime.

primarily manifested at a relatively higher q region. Similarly, the scattering signal at a lower q region is primarily due to a cylindrical arrangement of the polymer matrix. There is a sharp rise of the SAXS profile at a low q regime, which points to the existence of a mass fractal.

From the definition of the scattering vector (q) and Braggs law, q can be related to the length scale of the object as $d = 2\pi/q$. Before acid treatment, the poly(methacryloyl-DGA) matrix has an intercorrelated structure with a diameter of about 3.14 nm [$d = (2 \times 3.14)/2$ nm]. After acid treatment, the peak shifts toward higher q with a significant reduction in polydispersity. Figure 3d gives the normalized SAXS profiles for the poly(methacryloyl-DGA) samples before and after treatment with different HNO_3 concentrations. It is evident that the peak shifted to the same q value (q = 2.65 nm^{-1}) after treatment with both 1 and 4 mol L^{-1} HNO_3. Consequently, the diameter of the intercorrelated structure reduces to 2.37 nm. These two concentrations of HNO_3 studied were based on the fact that the $D_{Eu^{3+}}$ value significantly varied from 147 mL g^{-1} at 1 mol L^{-1} HNO_3 to ~4000 mL g^{-1} at 4 mol L^{-1} HNO_3. It is worth mentioning that, after acid treatment, the fractal structure of the poly(methacryloyl-DGA) matrix disappeared, as can be concluded from the low q regimes in Figure 3b and c. The poor statistics of Figure 3c may be attributed to the poor contrast effect upon treatment with 4 mol L^{-1} HNO_3. Due to the lack of exact knowledge about the complex enough morphology of the poly(methacryloyl-DGA) matrix, fitting of the SAXS profiles with a theoretical model would not give reliable results. However, from the changes in the SAXS profiles, it can unambiguously be concluded that acid treatment induces a geometrical arrangement of the poly(methacryloyl-DGA) matrix in the form of small assemblies in which the DGA units are in close proximity. Obviously, this will be due to hydrogen bonding caused by the sorption of HNO_3 molecules in the poly(methacryloyl-DGA) matrix. These hydrogen bonded assemblies act as strong binding sites for Am(III) and, consequently, are difficult to desorb, unless treated with EDTA at elevated temperature.[26] Heating will break the hydrogen bonded structure.

The monomeric DGA aggregate and polymeric DGA are different not only in terms of their physical assembling but also because of entropic considerations and internal degrees of freedom. Therefore, it was interesting to study their affinities toward different f-element ions as a function of the HNO_3 concentration. However, a direct comparison of the D values of the liquid−liquid extraction system with the liquid−solid extraction system is not possible due to the different dimensions (dimensionless and mL g^{-1}, respectively). To compare the extraction behavior of the monomeric and polymeric forms, the D_I values at different HNO_3 concentrations were normalized with the respective $D_{Am^{3+}}$ values at 3 mol L^{-1}, with this value being arbitrarily chosen. From Figure 4, it is clear that both the monomeric and polymeric extraction systems exhibit the same trend in their extraction behavior as a function of the HNO_3 concentration, being $D_{Eu^{3+}} > D_{Am^{3+}} \approx D_{Pu^{4+}} \gg D_{UO_2^{2+}}$. It is remarkable that both systems have almost

DOI: 10.1021/jp510170v
J. Phys. Chem. B 2015, 119, 212−218

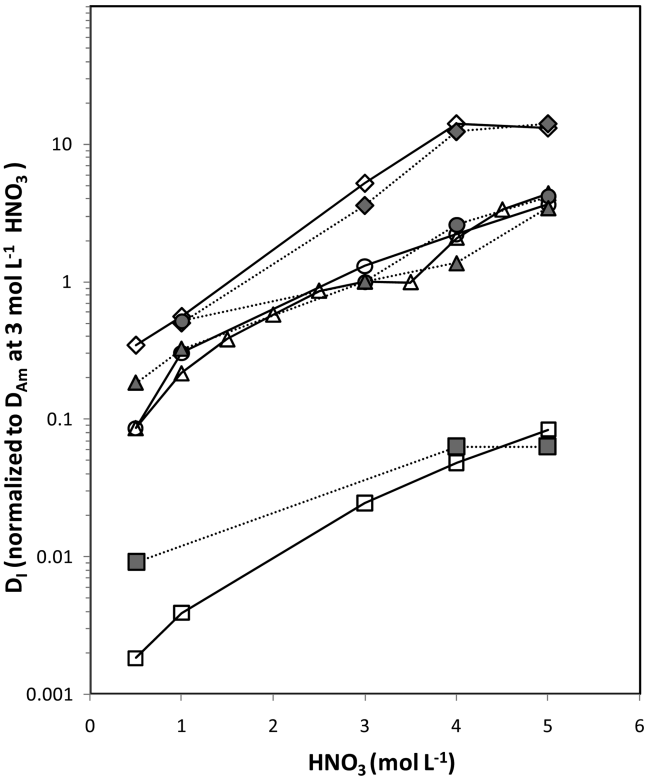

Figure 4. Normalized D_I values (I = Eu^{3+} (◇), Am^{3+} (△), Pu^{4+} (○), and UO_2^{2+} (□)) in systems consisting of aqueous:methacryloyl-DGA in organic phase (solid lines with unfilled symbols) and aqueous:poly-(methacryloyl-DGA) (broken lines with filled symbols) as a function of the HNO_3 concentration. The D_I values are normalized to the D_{Am} value at 3 mol L^{-1} HNO_3 of the respective system. The exact D_I values and their sources (present work or ref 26) are given in Table S1 (Supporting Information).

overlapping curves for a same f-element ion. In both systems, the $D_{Eu^{3+}}$ value increases more than that of other f-elements up to 4 mol L^{-1}, and saturates thereafter. This seems to suggest that both H-bonded DGA assemblies have a similar affinity toward f-element ions due to similar microscopic arrangements induced by HNO_3.

CONCLUSIONS

This study clearly demonstrates the utility of SAXS to give a better understanding of the extraction behavior of DGA-based ligands toward Ln/An(III) at higher acidities. Significant changes were observed in the geometrical arrangement of methacryloyl-DGA in an organic phase (10:1 mixture of *n*-dodecane and 1-decanol) and the poly(methacryloyl-DGA) matrix after treatment with HNO_3 bringing the DGA units in close proximity. The increase in the $D_{Am^{3+}}$ values as a function of the HNO_3 concentration in both the monomeric and polymeric forms of methacryloyl-DGA at constant nitrate concentration can be explained by the H-bond stabilization hypothesis of Qiao et al.[30] This study quantitatively shows that nitric acid-induced changes in elongation and swelling of DGA assemblies are due to an increase in H-bonds, which, in addition, also significantly influence the extraction behavior. For both the monomeric and polymeric methacryloyl-DGA, the normalized D values for a same f-element upon varying HNO_3 concentrations exhibit similar patterns, indicating that the microscopic arrangements induced by H-bonding would be similar. In both cases, the normal extraction mechanism is not operating as concluded from the unusual stoichiometry deduced from the slopes of the log D vs log[HNO_3] curves at a fixed nitrate ion concentration.

ASSOCIATED CONTENT

Supporting Information

Figures of SAXS profiles, a Porod plot, and a table containing distribution coefficients of Eu^{3+}, Am^{3+}, Pu^{4+}, and UO_2^{2+} in monomeric and polymeric methacryloyl-DGA. This material is available free of charge via the Internet at http://pubs.acs.org.

AUTHOR INFORMATION

Corresponding Authors

*Phone: +91 22 25594566. Fax: +91 22 25505151. E-mail: ashokk@barc.gov.in.

*Phone: +31 53489 2977. Fax: +31 53489 4645. E-mail: w.verboom@utwente.nl.

Author Contributions

The manuscript was written through contributions of all authors. All authors have given approval to the final version of the manuscript.

Notes

The authors declare no competing financial interest.

REFERENCES

(1) Ansari, S. A.; Pathak, P.; Mohapatra, P. K.; Manchanda, V. K. Chemistry of Diglycolamides: Promising Extractants for Actinide Partitioning. *Chem. Rev.* **2012**, *112*, 1751−1772.

(2) Sasaki, Y.; Tachimori, S. Extraction of Actinides (III),(IV),(V), (VI), and Lanthanides(III) by Structurally Tailored Diamides. *Solvent Extr. Ion Exch.* **2002**, *20*, 21−34.

(3) Cuillerdier, C.; Musikas, C.; Hoel, P.; Nigond, L.; Vitart, X. Malonamides as New Extractants for Nuclear Waste Solutions. *Sep. Sci. Technol.* **1991**, *26*, 1229−1244.

(4) Dam, H. H.; Verboom, W.; Reinhoudt, D. N. Multicoordinate Ligands for Actinide/Lanthanide Separations. *Chem. Soc. Rev.* **2007**, *36*, 367−377.

(5) Erlinger, C.; Gazeau, D.; Zemb, T.; Madic, C.; Lefrançois, L.; Hebrant, M.; Tondre, C. Effect of Nitric Acid Extraction on Phase Behavior, Microstructure and Interactions between Primary Aggregates in the System Dimethyldibutyltetradecylmalonamide (DMDBTDMA)/*n*-dodecane/water: a Phase Analysis and Small Angle X-Ray Scattering (SAXS) Characterisation Study. *Solvent Extr. Ion Exch.* **1998**, *16*, 707−738.

(6) Zhu, Z.-X.; Sasaki, Y.; Suzuki, H.; Suzuki, S.; Kimura, T. Cumulative Study on Solvent Extraction of Elements by *N,N,N′,N′*-tetraoctyl-3-oxapentanediamide (TODGA) from Nitric Acid into *n*-Dodecane. *Anal. Chim. Acta* **2004**, *527*, 163−168.

(7) Sasaki, Y.; Sugo, Y.; Suzuki, S.; Tachimori, S. The Novel Extractants, Diglycolamides, for the Extraction of Lanthanides and Actinides in HNO_3−*n*-dodecane System. *Solvent Extr. Ion Exch.* **2001**, *19*, 91−103.

(8) Ansari, S. A.; Pathak, P. N.; Manchanda, V. K.; Husain, M.; Prasad, A. K.; Parmar, V. S. *N,N,N′,N′*-Tetraoctyldiglycolamide (TODGA): A Promising Extractant for Actinide-Partitioning from High-Level Waste (HLW). *Solvent Extr. Ion Exch.* **2005**, *23*, 463−479.

(9) Sasaki, Y.; Rapold, P.; Arisaka, M.; Hirata, M.; Kimura, T.; Hill, C.; Cote, G. An Additional Insight into the Correlation between the Distribution Ratios and the Aqueous Acidity of the TODGA System. *Solvent Extr. Ion Exch.* **2007**, *25*, 187−204.

(10) Yaita, T.; Herlinger, A. W.; Thiyagarajan, P.; Jensen, M. P. Influence of Extractant Aggregation on the Extraction of Trivalent f-Element Cations by a Tetraalkyldiglycolamide. *Solvent Extr. Ion Exch.* **2004**, *22*, 553−571.

DOI: 10.1021/jp510170v
J. Phys. Chem. B 2015, 119, 212−218

(11) Ellis, R. J.; Audras, M.; Antonio, M. R. Mesoscopic Aspects of Phase Transitions in a Solvent Extraction System. *Langmuir* **2012**, *28*, 15498−15504.
(12) Ellis, R. J.; Anderson, T. L.; Antonio, M. R.; Braatz, A.; Nilsson, M. A SAXS Study of Aggregation in the Synergistic TBP−HDBP Solvent Extraction System. *J. Phys. Chem. B* **2013**, *117*, 5916−5924.
(13) Dourdain, S.; Hofmeister, I.; Pecheur, O.; Dufrêche, J.-F.; Turgis, R.; Leydier, A.; Jestin, J.; Testard, F.; Pellet-Rostaing, S.; Zemb, T. Synergism by Coassembly at the Origin of Ion Selectivity in Liquid−Liquid Extraction. *Langmuir* **2012**, *28*, 11319−11328.
(14) Ellis, R. J. Critical Exponents for Solvent Extraction Resolved Using SAXS. *J. Phys. Chem. B* **2014**, *118*, 315−322.
(15) Lefrançois, L.; Delpuech, J.-J.; Hébrant, M.; Chrisment, J.; Tondre, C. Aggregation and Protonation Phenomena in Third Phase Formation: an NMR Study of the Quaternary Malonamide/Dodecane/Nitric Acid/Water System. *J. Phys. Chem. B* **2001**, *105*, 2551−2564.
(16) Ellis, R. J.; Antonio, M. R. Coordination Structures and Supramolecular Architectures in a Cerium(III)−Malonamide Solvent Extraction System. *Langmuir* **2012**, *28*, 5987−5998.
(17) Ellis, R. J.; Meridiano, Y.; Chiarizia, R.; Berthon, L.; Muller, J.; Couston, L.; Antonio, M. R. Periodic Behavior of Lanthanide Coordination within Reverse Micelles. *Chem.—Eur. J.* **2013**, *19*, 2663−2675.
(18) Abécassis, B.; Testard, F.; Zemb, Th.; Berthon, L.; Madic, C. Effect of *n*-Octanol on the Structure at the Supramolecular Scale of Concentrated Dimethyldioctylhexylethoxymalonamide Extractant Solutions. *Langmuir* **2003**, *19*, 6638−6644.
(19) Jensen, M. P.; Yaita, T.; Chiarizia, R. Reverse-Micelle Formation in the Partitioning of Trivalent f-Element Cations by Biphasic Systems Containing a Tetraalkyldiglycolamide. *Langmuir* **2007**, *23*, 4765−4774.
(20) Nave, S.; Modolo, G.; Madic, C.; Testard, F. Aggregation Properties of *N,N,N′,N′*-tetraoctyl-3-oxapentanediamide (TODGA) in *n*-Dodecane. *Solvent Extr. Ion Exch.* **2004**, *22*, 527−551.
(21) Pathak, P. N.; Ansari, S. A.; Mohapatra, P. K.; Manchanda, V. K.; Patra, A. K.; Aswal, V. K. Role of Alkyl Chain Branching on Aggregation Behavior of Two Symmetrical Diglycolamides: Small Angle Neutron Scattering Studies. *J. Colloid Interface Sci.* **2013**, *393*, 347−351.
(22) Jańczewski, D.; Reinhoudt, D. N.; Verboom, W.; Hill, C.; Allignol, C.; Duchesne, M.-T. Tripodal Diglycolamides as Highly Efficient Extractants for f-Elements. *New J. Chem.* **2008**, *32*, 490−495.
(23) Iqbal, M.; Mohapatra, P. K.; Ansari, S. A.; Huskens, J.; Verboom, W. Preorganization of Diglycolamides on the Calix[4]arene Platform and its Effect on the Extraction of Am(III)/Eu(III). *Tetrahedron* **2012**, *68*, 7840−7847.
(24) Murillo, M. T.; Espartero, A. G.; Sánchez-Quesada, J.; de Mendoza, J.; Prados, P. Synthesis of Pre-Organized Bisdiglycolamides (bisDGA) and Study of their Extraction Properties for Actinides(III) and Lanthanides(III). *Solvent Extr. Ion Exch.* **2009**, *27*, 107−131.
(25) Mohapatra, P. K.; Ansari, S. A.; Iqbal, M.; Huskens, J.; Verboom, W. First Example of Diglycolamide-Grafted Resins: Synthesis, Characterization, and Actinide Uptake Studies. *RSC Adv.* **2014**, *4*, 10412−10419.
(26) Chavan, V.; Thekkethil, V.; Pandey, A. K.; Iqbal, M.; Huskens, J.; Meena, S. S.; Goswami, A.; Verboom, W. Assembled Diglycolamide for f-Element Ions Sequestration at High Acidity. *React. Funct. Polym.* **2014**, *74*, 52−57.
(27) Zemb, Th.; Taché, O.; Né, F.; Spalla, O. Improving Sensitivity of a Small Angle X-ray Scattering Camera with Pinhole Collimation using Separated Optical Elements. *Rev. Sci. Instrum.* **2003**, *74*, 2456−2462.
(28) Pederson, J. S. Analysis of Small-Angle Scattering Data from Colloids and Polymer Solutions: Modeling and Least Squares Fitting. *Adv. Colloid Interface Sci.* **1997**, *70*, 171−210.
(29) Teixeira, J. Small-Angle Scattering by Fractal Systems. *J. Appl. Crystallogr.* **1988**, *21*, 781−785.
(30) Qiao, B.; Demars, T.; Olverade la Cruz, M.; Ellis, R. J. How Hydrogen Bonds Affect the Growth of Reverse Micelles around Coordinating Metal Ions. *J. Phys. Chem. Lett.* **2014**, *5*, 1440−1444.

DOI: 10.1021/jp510170v
J. Phys. Chem. B 2015, 119, 212−218